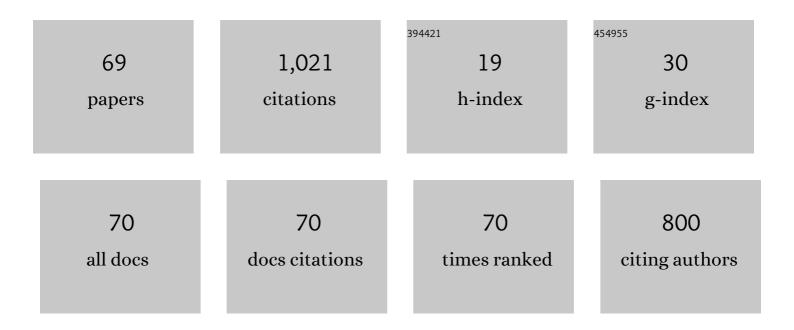
List of Publications by Year in descending order

Source: https://exaly.com/author-pdf/9151941/publications.pdf Version: 2024-02-01



#	Article	IF	CITATIONS
1	Ultra-precise determination of thicknesses and refractive indices of optically thick dispersive materials by dual-comb spectroscopy. Optics Express, 2022, 30, 2734.	3.4	1
2	Strain-induced irreversible change of the conductive network in a rubber/carbon-black composite revealed by polarization-resolved terahertz dielectric spectroscopy. Applied Physics Letters, 2022, 121, .	3.3	1
3	Ultra-Precise Complex Refractive Index Measurement Using Dual-Comb Spectroscopy. , 2021, , .		Ο
4	Interferogram-based determination of the absolute mode numbers of optical frequency combs in dual-comb spectroscopy. Optics Express, 2021, 29, 22214.	3.4	4
5	Evaluation of Crystallinity and Hydrogen Bond Formation in Stereocomplex Poly(lactic acid) Films by Terahertz Time-Domain Spectroscopy. Macromolecules, 2020, 53, 7171-7177.	4.8	24
6	Ultrafast coherent control of higher-order spin waves in a NiFe thin film by double-pulse excitation. Applied Physics Letters, 2020, 117, .	3.3	2
7	Terahertz time-domain polarimetry (THz-TDP) based on the spinning E-O sampling technique: determination of precision and calibration. Optics Express, 2020, 28, 13482.	3.4	19
8	Coherent Control of Higher-Order Spin Precession Modes in Ferromagnetic Permalloy Thin Films by Double Pulse Excitation. , 2020, , .		0
9	Internal Status of Visibly Opaque Black Rubbers Investigated by Terahertz Polarization Spectroscopy: Fundamentals and Applications. Polymers, 2019, 11, 9.	4.5	17
10	Real-Time Monitoring of Structural Changes in Poly(lactic acid) during Thermal Treatment by High-Speed Terahertz Time-Domain Spectroscopy for Nondestructive Inspection. ACS Applied Polymer Materials, 2019, 1, 3008-3016.	4.4	8
11	Development of Polarization-Sensitive Dual-Comb Spectroscopy for Anisotropic Materials. , 2019, , .		0
12	Polarization-Sensitive Electro-Optic Sampling of Elliptically-Polarized Terahertz Pulses: Theoretical Description and Experimental Demonstration. Particles, 2019, 2, 70-89.	1.7	1
13	Spatio-temporal imaging of terahertz electric-field vectors: observation of polarization-dependent knife-edge diffraction. Applied Physics Express, 2019, 12, 052010.	2.4	2
14	Polarization-sensitive dual-comb spectroscopy with an electro-optic modulator for determination of anisotropic optical responses of materials. Optics Express, 2019, 27, 35141.	3.4	6
15	Terahertz Sensing of Anisotropy in Polymeric Materials. The Review of Laser Engineering, 2019, 47, 21.	0.0	0
16	Ultrafast control of coherent spin precession in ferromagnetic thin films via thermal spin excitation processes induced by two-pulse laser excitation. Physical Review B, 2018, 97, .	3.2	10
17	Terahertz Polarization Imaging and Its Applications. Photonics, 2018, 5, 58.	2.0	35
18	Optical Response Change of Black Rubbers under Cyclic Deformation Investigated by Terahertz Polarization Spectroscopy. , 2018, , .		1

#	Article	IF	CITATIONS
19	Inspection of internal filler alignment in visibly opaque carbon-black–rubber composites by terahertz polarization spectroscopy in reflection mode. Polymer Testing, 2018, 72, 196-201.	4.8	13
20	Electric-Field Vector Imaging of Terahertz Surface Waves on an Indium Tin Oxide Thin Film. , 2018, , .		0
21	Magneto-optic Kerr effect CCD imaging with polarization modulation technique. AlP Advances, 2017, 7, 056802.	1.3	1
22	Controlled Terahertz Birefringence in Stretched Poly(lactic acid) Films Investigated by Terahertz Time-Domain Spectroscopy and Wide-Angle X-ray Scattering. Journal of Physical Chemistry B, 2017, 121, 6951-6957.	2.6	20
23	Anisotropic percolation conduction in elastomer-carbon black composites investigated by polarization-sensitive terahertz time-domain spectroscopy. Applied Physics Letters, 2017, 111, 221902.	3.3	13
24	Internal triaxial strain imaging of visibly opaque black rubbers with terahertz polarization spectroscopy. APL Photonics, 2017, 2, .	5.7	17
25	Detailed study of transient anomalous electric field vector focused by parabolic mirror. Journal of Optics (United Kingdom), 2017, 19, 035603.	2.2	3
26	Polarization-sensitive dual-comb spectroscopy. Journal of the Optical Society of America B: Optical Physics, 2017, 34, 154.	2.1	15
27	Retrieving the undistorted terahertz time-domain electric-field vector from the electro-optic effect. Journal of the Optical Society of America B: Optical Physics, 2017, 34, 1946.	2.1	6
28	Anisotropic optical response of optically opaque elastomers with conductive fillers as revealed by terahertz polarization spectroscopy. Scientific Reports, 2016, 6, 39079.	3.3	32
29	Polarization-sensitive electro-optic detection of terahertz wave using three different types of crystal symmetry: Toward broadband polarization spectroscopy. Applied Physics Letters, 2016, 108, .	3.3	14
30	Birefringent properties of poly-lactic acid at terahertz range. , 2016, , .		0
31	Spatial polarization variation in terahertz electromagnetic wave focused by off-axis parabolic mirror. Applied Physics Express, 2016, 9, 052206.	2.4	12
32	Intrinsic formation of electromagnetic divergence and rotation by parabolic focusing. Physical Review A, 2015, 92, .	2.5	11
33	Time-domain picture of the terahertz vector waveform measured by the electro-optic sampling method using the crystal symmetry. , 2014, , .		Ο
34	Video-rate terahertz electric-field vector imaging. Applied Physics Letters, 2014, 105, 151103.	3.3	7
35	Polarization detection of terahertz radiation via the electro-optic effect using zinc blende crystal symmetry. Journal of the Optical Society of America B: Optical Physics, 2014, 31, 3170.	2.1	7
36	High-speed terahertz time-domain polarimeter based on an electro-optic modulation technique. Applied Physics Express, 2014, 7, 092401.	2.4	23

#	Article	IF	CITATIONS
37	A Real-Time Terahertz Time-Domain Polarization Analyzer with 80-MHz Repetition-Rate Femtosecond Laser Pulses. Sensors, 2013, 13, 3299-3312.	3.8	12
38	Terahertz electric-field vector camera. , 2013, , .		0
39	Robustness of electric field vector sensing of electromagnetic waves by analyzing crystal angle dependence of the electro-optic effect. Journal of the Optical Society of America B: Optical Physics, 2013, 30, 2940.	2.1	10
40	T-ray topography by time-domain polarimetry. Optics Letters, 2012, 37, 2706.	3.3	23
41	Precise real-time polarization measurement of terahertz electromagnetic waves by a spinning electro-optic sensor. Review of Scientific Instruments, 2012, 83, 023104.	1.3	50
42	Terahertz profilometer by time-domain polarimetry. , 2012, , .		0
43	Intense Terahertz Pulse-Induced Nonlinear Responses in Carbon Nanotubes. Journal of Infrared, Millimeter, and Terahertz Waves, 2012, 33, 861-869.	2.2	26
44	Intense terahertz pulse induced exciton generation in carbon nanotubes. Optics Express, 2011, 19, 1528.	3.4	73
45	Intense terahertz pulse induced exciton generation in carbon nanotubes: erratum. Optics Express, 2011, 19, 15388.	3.4	3
46	Ultrafast photo-induced insulator-to-metal transition in the spin density wave system of (TMTSF)2PF6. Physica B: Condensed Matter, 2010, 405, S360-S362.	2.7	1
47	Intense terahertz field-induced electroabsorption in carbon nanotubes. , 2010, , .		0
48	Room temperature terahertz electro-optic modulation by excitons in carbon nanotubes. Applied Physics Letters, 2010, 97, 041111.	3.3	21
49	Observation of ultrafast photoinduced closing and recovery of the spin-density-wave gap in(TMTSF)2PF6. Physical Review B, 2009, 80, .	3.2	12
50	Spinâ€densityâ€wave gap in (TMTSF) <sub>2</sub> PF <sub>6</sub> probed by reflectionâ€type terahertz timeâ€domain spectroscopy. Physica Status Solidi (B): Basic Research, 2008, 245, 2688-2691.	1.5	8
51	Compact terahertz time domain spectroscopy system with diffraction-limited spatial resolution. Review of Scientific Instruments, 2007, 78, 103906.	1.3	7
52	Very compact THz-TDS imaging system with diffraction limited spatial resolution. , 2007, , .		0
53	Narrow (â‰^4meV) inhomogeneous broadening and its correlation with confinement potential of pyramidal quantum dot arrays. Applied Physics Letters, 2007, 91, 081106.	3.3	29
54	Mechanisms of Quantum Dot Energy Engineering by Metalorganic Vapor Phase Epitaxy on Patterned Nonplanar Substrates. Nano Letters, 2007, 7, 1282-1285.	9.1	51

#	Article	IF	CITATIONS
55	Patterning of confined-state energies in site-controlled semiconductor quantum dots. Applied Physics Letters, 2005, 86, 243105.	3.3	11
56	Dense uniform arrays of site-controlled quantum dots grown in inverted pyramids. Applied Physics Letters, 2004, 84, 2907-2909.	3.3	50
57	Growth and optical characterization of dense arrays of site-controlled quantum dots grown in in inverted pyramids. Physica E: Low-Dimensional Systems and Nanostructures, 2004, 21, 193-198.	2.7	4
58	Site-controlled quantum dots grown in inverted pyramids for photonic crystal applications. Physica E: Low-Dimensional Systems and Nanostructures, 2004, 23, 476-481.	2.7	23
59	Site- and energy-controlled pyramidal quantum dot heterostructures. Physica E: Low-Dimensional Systems and Nanostructures, 2004, 25, 288-297.	2.7	40
60	High uniformity of site-controlled pyramidal quantum dots grown on prepatterned substrates. Applied Physics Letters, 2004, 84, 1943-1945.	3.3	79
61	High-quality InxGa1–xAs/Al0.30Ga0.70As quantum dots grown in inverted pyramids. Physica Status Solidi (B): Basic Research, 2003, 238, 233-236.	1.5	27
62	Vertically polarized lasing and photoluminescence in a ridge quantum-wire laser. Physical Review B, 2003, 68, .	3.2	1
63	Imaging of emission patterns in a T-shaped quantum wire laser. Applied Physics Letters, 2003, 83, 4089-4091.	3.3	10
64	Lasing from a single-quantum wire. Applied Physics Letters, 2002, 81, 4937-4939.	3.3	58
65	Polarization Dependence of the Optical Interband Transition Defined by the Spatial Variation of the Valencep-Orbital Bloch Functions in Quantum Wires. Japanese Journal of Applied Physics, 2002, 41, 5924-5936.	1.5	7
66	Transformation of GaAs (001)–(111)B facet structure by surface diffusion during molecular beam epitaxy on patterned substrates. Journal of Crystal Growth, 2001, 227-228, 62-66.	1.5	5
67	Microscopy of electronic states contributing to lasing in ridge quantum-wire laser structure. Applied Physics Letters, 1999, 75, 2190-2192.	3.3	8
68	Selective molecular beam epitaxy (MBE) growth of GaAs/AlAs ridge structures containing 10nm scale wires and side quantum wells (QWs) and their stimulated emission characteristics. Journal of Crystal Growth, 1999, 201-202, 810-813.	1.5	13
69	Stimulated emission in ridge quantum wire laser structures measured with optical pumping and microscopic imaging methods. Applied Physics Letters, 1998, 73, 511-513.	3.3	33